3D-Var and 4D-Var approaches to ocean data assimilation

Anthony T. Weaver

CERFACS
42 avenue Gaspard Coriolis
31057 Toulouse Cedex 1
France
weaver@cerfacs.fr

ABSTRACT

Three- and four-dimensional variational (3D-Var and 4D-Var) approaches to ocean data assimilation are discussed. Particular examples are taken from a variational assimilation system developed for the OPA ocean general circulation model. 4D-Var is shown to be globally superior to 3D-Var. There is considerable scope for improving the current 3D-Var system, however. The background-error covariances are identified as a critical area where significant improvement can be made to 3D-Var (and possibly 4D-Var). The cost benefits of 4D-Var versus 3D-Var should be carefully re-evaluated when improved versions of 3D-Var become available.

1   Introduction

Variational data assimilation systems are operational in most major Numerical Weather Prediction (NWP) centres (Parrish and Derber 1992; Courtier *et al.* 1998; Gauthier *et al.* 1999; Rabier *et al.* 2000; Lorenc *et al.* 2000). Variational assimilation overcomes many of the limitations of optimal interpolation (OI) which was the standard technique used for many years in NWP (Gandin 1965; Rutherford 1972; Lorenc 1981) and variants of which are still widely used in operational ocean data assimilation systems (Smith *et al.* 1991; Bell *et al.* 2000; De Mey and Benikran 2001; Segschneider *et al.* 2002). Compared to OI, variational assimilation allows for greater flexibility for assimilating different observation types (possibly nonlinearly related to the model state); it eliminates the need to split the analysis domain into subsections so that all observations can in principle influence the analysis at every model grid-point; it provides a more general framework for using more sophisticated background-error covariance models; and it provides a clearer development path towards advanced, four-dimensional assimilation techniques. These advantages are relevant for ocean as well as atmospheric data assimilation.

In this paper, we describe three- and four-dimensional variational assimilation (3D-Var and 4D-Var) systems (Weaver *et al.* 2003) that have been developed for the OPA Ocean General Circulation Model (OGCM) of the Laboratoire d'Océanographie Dynamique et de Climatologie (LODYC; Madec *et al.* 1998). The purpose of this paper is to discuss some of the important distinguishing features of each system and to identify important avenues of research for improving the systems. This paper borrows heavily from material presented in recent articles by Weaver *et al.* (2003) and Vialard *et al.* (2003).

2 Incremental formulations of 3D-Var and 4D-Var

We first present the complete 4D-Var problem before describing its incremental variant. We define $\mathbf{y}^o = (...,(\mathbf{y}_i^o)^T,...)^T$ to be the vector of observations available over a time window $t_0 \leq t_i \leq t_n$ where $\mathbf{y}_i^o$ corresponds to the observation vector at time t_i. We define $\mathbf{x}^b$ to be the background estimate of the ocean initial state vector $\mathbf{x} = \mathbf{x}(t_0)$ at the beginning of the window. The basic principle of 4D-Var is then to compute the initial state vector $\mathbf{x}$ that leads to the best simultaneous fit, in a statistically-weighted least-squares sense, to $\mathbf{y}^o$ and to $\mathbf{x}^b$. The problem is defined by the minimization of a cost function $J(\mathbf{x}) = J_b + J_o$ where

$$J_b = \frac{1}{2}\left(\mathbf{x} - \mathbf{x}^b\right)^T \mathbf{B}^{-1} \left(\mathbf{x} - \mathbf{x}^b\right); \tag{1}$$

$$J_o = \frac{1}{2}\left(G(\mathbf{x}) - \mathbf{y}^o\right)^T \mathbf{R}^{-1} \left(G(\mathbf{x}) - \mathbf{y}^o\right). \tag{2}$$

$G(\cdot)$ is a generalized observation operator that computes the model equivalent of the observation vector $\mathbf{y}^o$ from $\mathbf{x}$; it includes an integration of the nonlinear model from initial time to the observation times within the assimilation window, followed by an interpolation to the observation points. The matrices $\mathbf{B}$ and $\mathbf{R}$ contain estimates of the background- and observation-error covariances, respectively.

The incremental formulation of 4D-Var (Courtier *et al.* 1994) is a variant of the full problem above, and was introduced in operational meteorology to overcome some important practical difficulties with solving the complete problem directly. Incremental 4D-Var is defined by the minimization of a sequence, $k = 1, ..., K$, of quadratic cost functions $J^k(\delta\mathbf{x}^k) = J_b + J_o^k$ where

$$J_b = \frac{1}{2}\left(\delta\mathbf{x}^k - \mathbf{x}^b + \mathbf{x}^{k-1}\right)^T \mathbf{B}^{-1} \left(\delta\mathbf{x}^k - \mathbf{x}^b + \mathbf{x}^{k-1}\right); \tag{3}$$

$$J_o^k = \frac{1}{2}\left(\mathbf{G}^{k-1}\delta\mathbf{x}^k - \mathbf{d}^{k-1}\right)^T \mathbf{R}^{-1} \left(\mathbf{G}^{k-1}\delta\mathbf{x}^k - \mathbf{d}^{k-1}\right). \tag{4}$$

$\delta\mathbf{x}^k = \mathbf{x}^k - \mathbf{x}^{k-1}$ defines an increment to a reference state $\mathbf{x}^{k-1}$ with $\mathbf{x}^0 = \mathbf{x}^b$; $\mathbf{d}^{k-1} = \mathbf{y}^o - G(\mathbf{x}^{k-1})$ is the vector of observation-minus-reference state differences (this difference equal to the innovation vector when $k = 1$); and $\mathbf{G}^{k-1} \approx \partial G/\partial\mathbf{x}|_{\mathbf{x}=\mathbf{x}^{k-1}}$ is a linear operator defined with respect the basic state $\mathbf{x}^{k-1}$. $\mathbf{G}^{k-1}$ contains an integration of the tangent-linear model (usually simplified to eliminate nonsmooth parametrisations) from initial time to the observation times. The simplification in the incremental problem is made in the observation term (4), which now becomes quadratic compared to the nonquadratic formulation in (2). Gradient descent methods such as conjugate gradient are efficient algorithms for minimizing quadratic functions (e.g., see Nocedal and Wright 1999). The adjoint of the linearized operator $\mathbf{G}^{k-1}$ is used to compute the gradient of J_o^k with respect to $\delta\mathbf{x}^k$. Nonlinearities in $G(\cdot)$ are accounted for through the outer iterations (the sequence $k = 1, ..., K$) by allowing the basic state of the linear operator $\mathbf{G}^{k-1}$ (and its adjoint $(\mathbf{G}^{k-1})^T$) to be updated with a more recent estimate of $\mathbf{x}$ obtained during minimization. In both the full and incremental formulations, the background term (Eqs. (1) and (3)) is identical.

An incremental version of 3D-Var can be derived as a limiting case of incremental 4D-Var by replacing the tangent-linear operator in $\mathbf{G}^{k-1}$ with the identity matrix; i.e., we assume that increments at initial time persist for the duration of the assimilation window. Observations are still assimilated at their appropriate measurement times by comparing them with the reference state at those times in order to form the difference vector $\mathbf{d}^{k-1}$. This version of 3D-Var is known as FGAT for First-Guess at Appropriate Time (Fisher and Andersson 2001) in contrast to more classical implementations of 3D-Var which often treat time-distributed observations simultaneously during assimilation.

Incremental 4D-Var should be viewed as a practical algorithm for solving the complete 4D-Var problem. Incremental 3D-Var, on the other hand, is only a valid approximation to 4D-Var when the model dynamics

are quasi-stationary and thus in the limit of very short assimilation windows. The FGAT version of 3D-Var is nonetheless an improvement over classical 3D-Var since it eliminates a component of mean analysis error that can arise when comparing observations and a model background which are valid at different times (Fisher and Andersson 2001).

3 Examples from 3D-Var and 4D-Var systems for OPA

The results presented here have been produced using 3D-Var and 4D-Var systems (Weaver *et al.* 2003) developed for a rigid-lid version of the OPA OGCM (Madec *et al.* 1998). The model configuration covers the tropical Pacific basin (Vialard *et al.* 2001). The observations used for assimilation are subsurface temperature measurements from a quality controlled version of the Global Temperature and Salinity Pilot Project data-set of the National Oceanographic Data Centre.

3.1 Tangent-linear versus persistence

The fundamental difference between 3D-Var and 4D-Var lies in the sophistication of the linear model used to transport the increment from initial time to the observation times within the assimilation window. The accuracy of the linear models (persistence for 3D-Var; the tangent-linear model for 4D-Var) can be assessed by comparing the time-evolution of an initial perturbation in the nonlinear model with its evolution in the linear model. Figure 1a shows a vertical section at 110°W of the difference between a 4D-Var analysis and the background state valid at the same time. This perturbation is roughly representative of the structure and amplitude of increments generated by the assimilation system. The perturbations after 10 and 30 days of integration in the nonlinear model are shown in Figs. 1b and c, respectively. Ten days is the window width used in our 3D-Var system and is typical of window widths used in other 3D ocean assimilation systems (e.g., Segschneider *et al.* 2002). Figures 1a and b allow us to verify the assumption in 3D-Var that perturbations evolve slowly over 10 days. The large amplitude anomalies in the off-equatorial regions are indeed well approximated by persistence. The persistence assumption breaks down nearer the equator, however, where the ocean dynamical response is much more rapid. In contrast, Figs. 1c and d show that the tangent-linear model is able to provide a good description of the perturbation in both equatorial and off-equatorial regions at least 30 days ahead. A 30-day window width has been used for the 4D-Var experiments presented here. It is not clear if this is the best choice. For example, longer windows would be preferable to make better nonlocal use of ocean observations. However, longer windows also introduce greater limitations on the validity of the tangent-linear approximation, particularly at the small scales (e.g., tropical instability waves), and of the perfect model assumption implicit in 4D-Var.

3.2 Flow-dependent background-error variances

It is well known that, in the limit of a perfect, linear model, variational assimilation is equivalent to the Kalman filter in that, given identical inputs, they produce the same analysis at the end of the assimilation window (e.g., see Courtier *et al.* 1994). By exploiting this theoretical equivalence, it is possible to diagnose flow-dependent features of the time-evolved background-error covariances that are computed implicitly in the variational minimization algorithm (e.g., Thépaut *et al.* 1996).

Figure 2, left panel, shows vertical profiles of the background-error standard deviations σ^b for temperature at the equator in the central Pacific (140°W). The dashed-dotted curve is the prior value of σ^b, which has been estimated, albeit rather crudely, from the model climatology in an experiment without data assimilation.
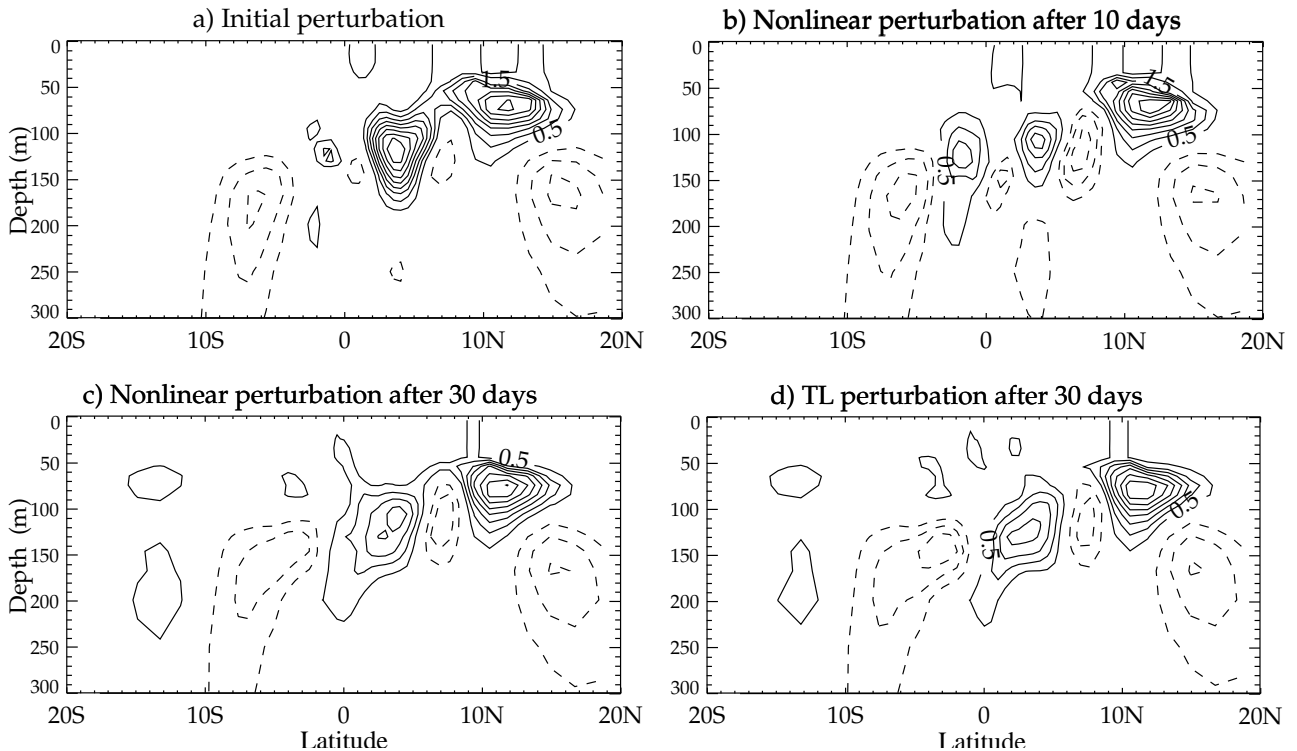
Figure 1: a) Vertical section at 110°W of a temperature perturbation defined as the difference between a 4D-Var analysis and the background state valid at the same time. The perturbation after b) 10 days and c) 30 days evolution in the nonlinear model, and after d) 30 days evolution in the tangent-linear model. The contour interval is 0.5°C.

It has a rather broad structure throughout the upper ocean and displays a maximum around the depth of the climatological thermocline (near 170m). In 3D-Var these σ^b are effectively used to weight the background state at all times within the assimilation window, whereas in 4D-Var they are used to weight the background state only at the beginning of the window. The solid curve in Fig. 2, left panel, shows an example of the effective σ^b used in 4D-Var at the end of a 30-day window. The tangent-linear dynamics tend to reduce the σ^b in the mixed layer and to sharpen the profile around the level of maximum background-error variance. The maximum occurs at the level of the thermocline as confirmed by comparing σ^b to a corresponding 30-day mean profile of the background $|\partial T/\partial z|$ (Fig. 2, right panel). This tendency is physically sensible since the level of maximum variability of the thermal field, and thus of maximum likely error, is located at the level of the thermocline.

3.3 Fit to the observations

Statistics derived from the background-minus-observation vector (BmO $\equiv G(\mathbf{x}^b) - \mathbf{y}^o$) and analysis-minus-observation vector (AmO $\equiv G(\mathbf{x}^a) - \mathbf{y}^o$) can yield useful information about the internal consistency of the data assimilation system (Hollingsworth and Lönnberg 1989). Figures 3a and b shows the root-mean-square (rms) of the BmO and AmO as a function of depth for all buoy data from the Tropical Atmosphere Ocean (TAO) array assimilated in 3D-Var and 4D-Var experiments cycled over the period 1993-98. The rms of the "BmO" of a control experiment, in which no data are assimilated, is also shown. The control shows large differences both just below the thermocline, where there are large biases, and in the thermocline, where signals associated with the seasonal cycle and interannual variability are largest. These differences are substantially reduced in
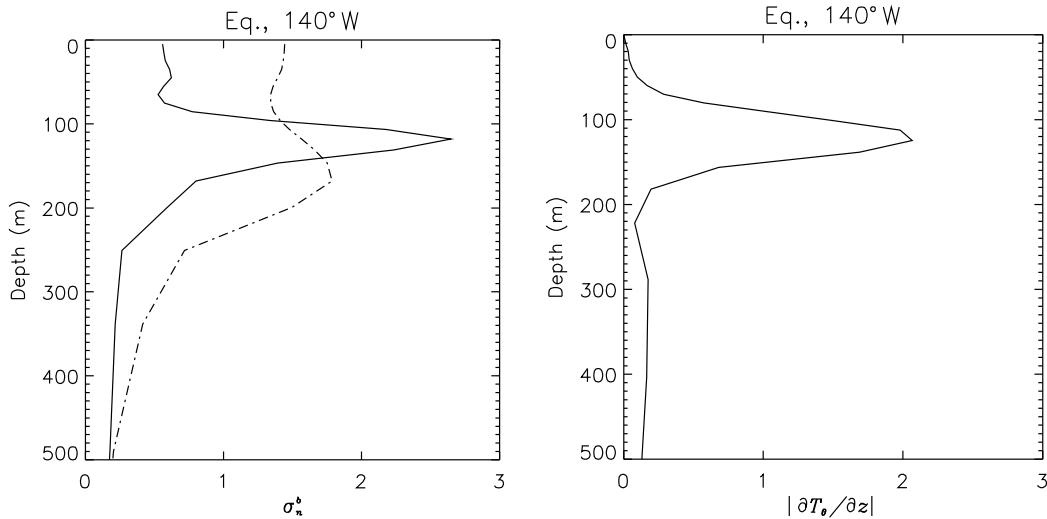
Figure 2: Left panel: vertical profiles of the background-error standard deviations (in °C) used in 3D-Var and 4D-Var at the equator at 140°W. The dashed-dotted curve corresponds to the standard deviations specified at the beginning of the assimilation window. In 3D-Var, these are also the effective standard deviations used at all future times within the window. The solid curve corresponds to the effective standard deviations used implicitly in 4D-Var at the end of the 30-day window in a particular cycle of 4D-Var. Right panel: the corresponding profile of the background $|\partial T/\partial z|$ at this location. The values of $|\partial T/\partial z|$ have been multiplied by a factor of ten in order to be plotted with the same horizontal scale as in panel a.

3D-Var and 4D-Var. The rms of the BmO in 4D-Var is similar to that of 3D-Var, with a maximum around 1.5°C at the level of the thermocline. On the other hand, the rms of the AmO in 4D-Var is very much reduced, being less than 0.5°C over the entire water column, compared to the rms of AmO in 3D-Var which is hardly smaller than that of the BmO. The fit to the TAO data in 4D-Var is within the specified level of observation error (0.5°C), which is not the case in 3D-Var.

The larger AmO in 3D-Var is in fact primarily an artifact of the "initialization" procedure used in 3D-Var. An initialization scheme was necessary since, due to the univariate formulation of **B**, the 3D-Var analysis increment was for temperature only and thus not balanced. A simple scheme based on incremental updating (Bloom *et al.* 1996) was applied to allow the model to adjust gradually to the analysis increment. While minimizing initialization shocks, this procedure ultimately degrades the fit to the data achieved by the static 3D-Var analysis. This is illustrated in Fig. 3b which shows that for 3D-Var the rms of the J_o^k residual $\mathbf{G}^{k-1}\delta\mathbf{x}^a - \mathbf{d}^{k-1}$, is considerably less than the AmO (but still greater than the AmO of 4D-Var) and is comparable to the specified standard deviation of observation error (0.5°C). No outer iterations ($K = 1$) were used in 3D-Var since all operators are linear and independent of the basic state.

In contrast to the 3D-Var, 4D-Var produces a multivariate analysis of temperature, salinity and currents. No initialization procedure was used in 4D-Var; the analysis increment was added directly to the background state. The residual and AmO for 4D-Var, shown in Fig. 3b, are indistinguishable. This result demonstrates that the full and incremental cost functions converge to similar values in 4D-Var, and thus provides a good measure of the consistency of the incremental approach for solving the full problem. In these 4D-Var experiments, five outer iterations ($K = 6$) were performed every 10 iterations of the minimization.
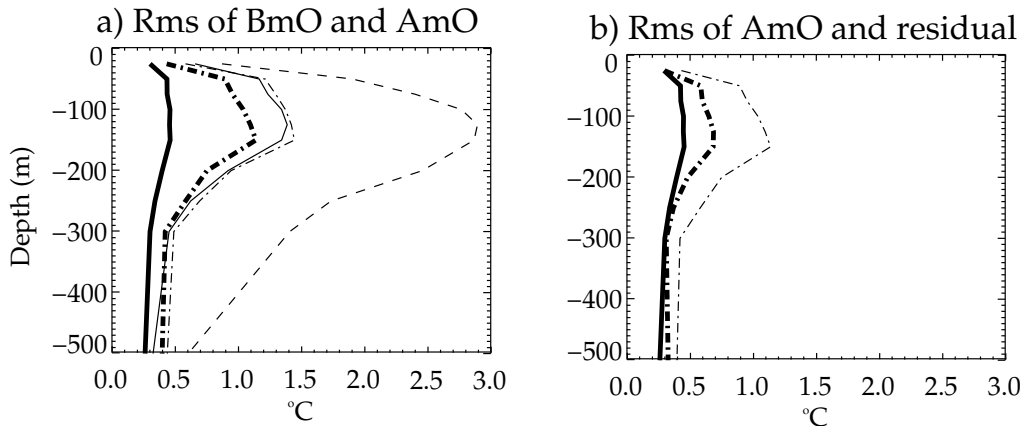
Figure 3: Time-averaged statistics, plotted as a function of depth, of BmO and AmO for TAO data during the 1993-98 period. a) The rms of BmO (thin curves) and AmO (thick curves); and b) the rms of AmO (thin curves) and of the J_o^k residual (thick curves). In panel a, the dashed curve corresponds to the control; in both panels, the dashed-dotted curves correspond to 3D-Var, and the solid curves to 4D-Var. The AmO and J_o^k residual of 4D-Var (solid curves in panel b) are indistinguishable.

3.4   Evidence of bias

The long-term average of the analysis increments can be used to assess the presence of bias in the assimilation system. If the system is unbiased then the time-averaged increments should be zero. Figure 4b shows the average profile of temperature (panel a) and of the analysis increment (panel b). produced by 3D-Var and 4D-Var in the Niño3 region (150°W–90°W, 5°S–5°N). It can be seen that, while the mean thermal profiles in 3D-Var and 4D-Var are very similar, the mean analysis increments are very different. In 4D-Var, the mean analysis increment has an intuitive effect; it generally acts systematically to heat the upper part of the thermocline and to cool its lower part, thus counteracting the tendency of the model to spread the thermocline (Vialard *et al.* 2003). In 3D-Var, the analysis increments cool rather strongly the entire thermocline. The quite different vertical structure of the mean analysis increments in 3D-Var compared to those in 4D-Var is in fact linked to a spurious circulation cell that develops in the univariate 3D-Var analysis but not in the 4D-Var analysis. As a result, the analysis increments in 3D-Var tend to mainly correct for a bias created by the 3D-Var analysis itself, whereas in 4D-Var they tend to correct for a bias present in the control.

3.5   Variability

One of the main advantages of 4D-Var over 3D-Var is its ability to make better synergetic use of sequential observations. An example is presented here to show how 4D-Var is able to accurately reproduce variability in the data occurring on time-scales comparable to or less than the width of the assimilation window. Figure 5 shows the daily depth of the 20°C isotherm (D20) at (140°W, 5°N) from TAO data and from the 3D-Var, 4D-Var and control experiments. The large oscillations, up to 60m from peak to trough, with periods between 30 and 40 days, are associated with tropical instability waves (TIWs). TIWs are the largest contributor to variability in the tropical Pacific at intraseasonal time-scales. There is no TIW activity during the April-to-June period.

The control does not exhibit clear TIW variability at this location. The TIW variability is slightly stronger in 3D-Var, but the amplitude is underestimated and there is a phase lag behind observations. In 4D-Var, however, the TIWs are reproduced with the correct phase and amplitude. The only significant misfit between 4D-Var and the data is observed in early February and lasts only a few days. This implies that 4D-Var is able to fit
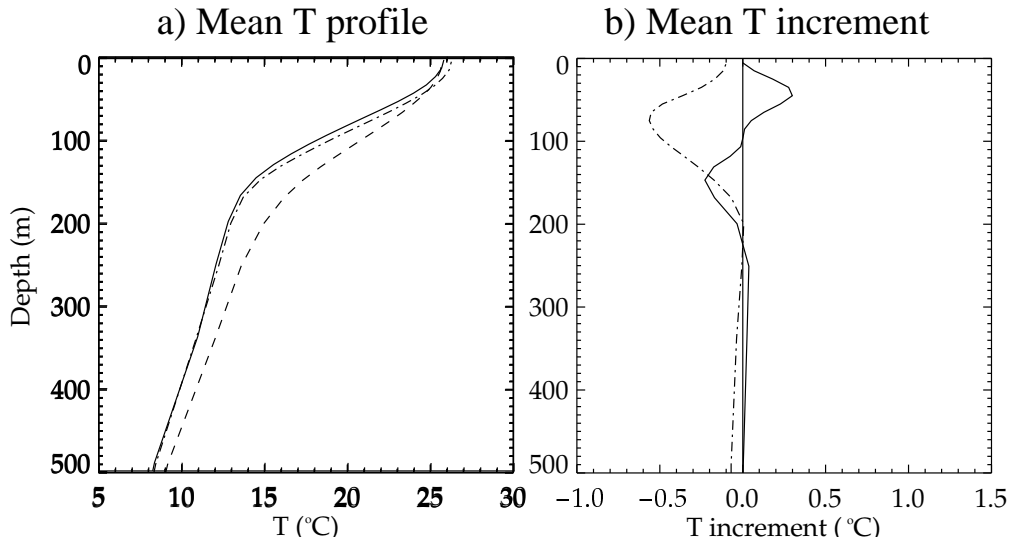
Figure 4: The 1993-96 average temperature a) profile and b) analysis increment in the Niño3 region. 4D-Var is displayed with a solid curve, 3D-Var with a dashed-dotted curve and the control with a dashed curve.

variability in the data having a time-scale shorter than the 30-day assimilation window.

The D20 trajectory of the 4D-Var is smooth in the sense that there are no significant "jumps" at analysis time when the increment is applied. This is also true of 3D-Var because the initialization procedure based on incremental updating acts as a low-pass time filter (Bloom *et al.* 1996). This smoothness of the 3D-Var analysis, however, is achieved at the expense of resolving accurately TIW activity as illustrated in Fig. 5. Whereas the static linear analysis $G(\mathbf{x}^{k-1}) + \mathbf{G}^{k-1}\delta\mathbf{x}^a$ of 3D-Var reproduces quite well the D20 variations associated with the TIWs, the updated trajectory does not fit these variations as well.

4   Final comments and avenues for improvement

Comparisons of 3D-Var and 4D-Var analyses in the tropical Pacific indicate that 4D-Var is superior to 3D-Var in several areas. The fit to the assimilated temperature observations is consistently better in 4D-Var than in 3D-Var. Furthermore, the impact on those state variables (horizontal currents and salinity) not directly observed is generally better in 4D-Var than in 3D-Var (Vialard *et al.* 2003). One of the distinguishing features of the 3D-Var analyses is a large bias in the velocity field which is associated with a spurious circulation cell that develops along the equatorial strip (strong downwelling in the east Pacific, weaker but broader upwelling in the central/west Pacific, eastward surface currents). This bias is also present in the temperature field but is greatly reduced on each assimilation cycle by the direct assimilation of subsurface temperature data.

Many of the deficiencies with the 3D-Var analyses are not fundamental to 3D-Var but can be attributed to an inadequate treatment of the background error covariances. This is an area where significant improvements can be made to 3D-Var (and possibly 4D-Var) and where much of the current research effort is being directed in the CERFACS data assimilation group. The univariate treatment of the background error covariances is obviously a weak point and is one of the suspected reasons for the large bias that develops in the 3D-Var analyses. Recently, a multivariate formulation of the background error covariance matrix has been developed to include constraints between temperature and salinity, and between density and currents. Some of these constraints (e.g., between temperature and salinity) are fundamentally nonlinear (cf. Troccoli *et al.* 2002) and thus must
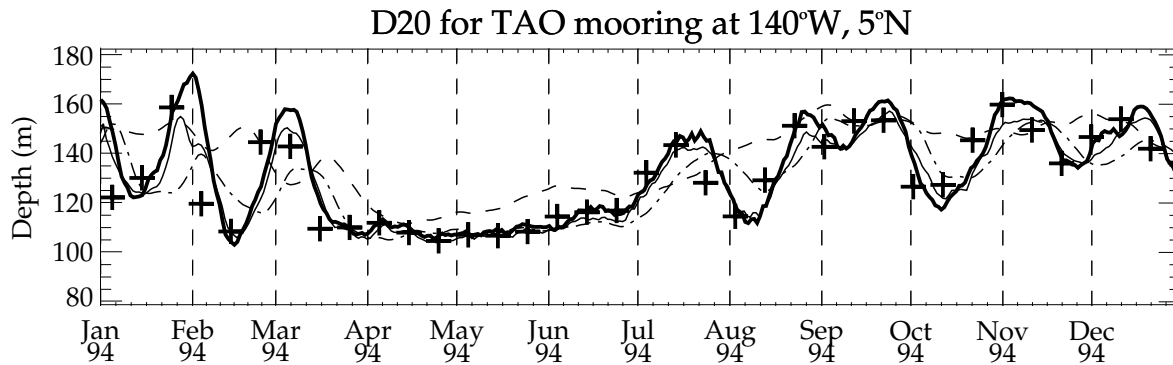
Figure 5: Time-series of the daily averaged D20 during 1994 at (140°W, 5°N). The thick curve is the (assimilated) TAO in situ data. The solid curve corresponds to 4D-Var, the dashed-dotted curve to 3D-Var, and the dashed curve to the control. All time-series have been smoothed using a 5-day sliding average. The crosses indicate the D20 of 3D-Var computed at the observation points from the static analysis $G(\mathbf{x}^{k-1}) + \mathbf{G}^{k-1}\delta\mathbf{x}^a$. The dashed-dotted curve corresponds to the updated model trajectory obtained using the incremental updating scheme.

be linearized to be implemented within a covariance matrix. Linearization is performed with respect to the background state. This allows the constraints to evolve from one assimilation cycle to the next and thus to take into account the impact of data assimilation from previous cycles in deriving the covariances for the current cycle. The covariances for the horizontal currents are constrained using a geostrophic relation that combines a β-plane approximation near the equator with an f-plane approximation away from the equator (Burgers *et al.* 2002; Balmaseda 2003). A flow-dependent parametrisation has also been introduced for the background-error variances. Inspired by the results from Fig. 2, we have made the background-error variances dependent on the vertical gradient of the background state. Figure 6c shows the impact of the improved (multivariate, flow-dependent) covariance model in 3D-Var on the climatology of the equatorial surface currents. For comparison, Fig. 6b shows the same climatology for a 3D-Var experiment with the original (univariate, flow-independent) covariance model, and Fig. 6a shows the observed climatology from Reverdin *et al.* (1994). A notable feature in Fig. 6b is the large eastward bias in the equatorial surface currents, as already pointed out above. A similar bias is also present in other univariate assimilation systems (for a discussion see Balmaseda 2003). The main impact of the improved covariances in 3D-Var is to eliminate this eastward bias and bring the currents much closer to the observed climatology.

An effective variational assimilation system requires substantial development and tuning. The results above illustrate, for example, how improved background error covariance models can have a significant impact on the quality of 3D-Var analyses. The extent to which these improved covariance models can impact the quality of 4D-Var analyses remains to be evaluated. It also remains to be seen how the relative difference in quality between 3D-Var and 4D-Var analyses will change as the system evolves to incorporate additional data (e.g., sea level from altimetry, salinity from Argo floats) and better background- and observation-error covariances.
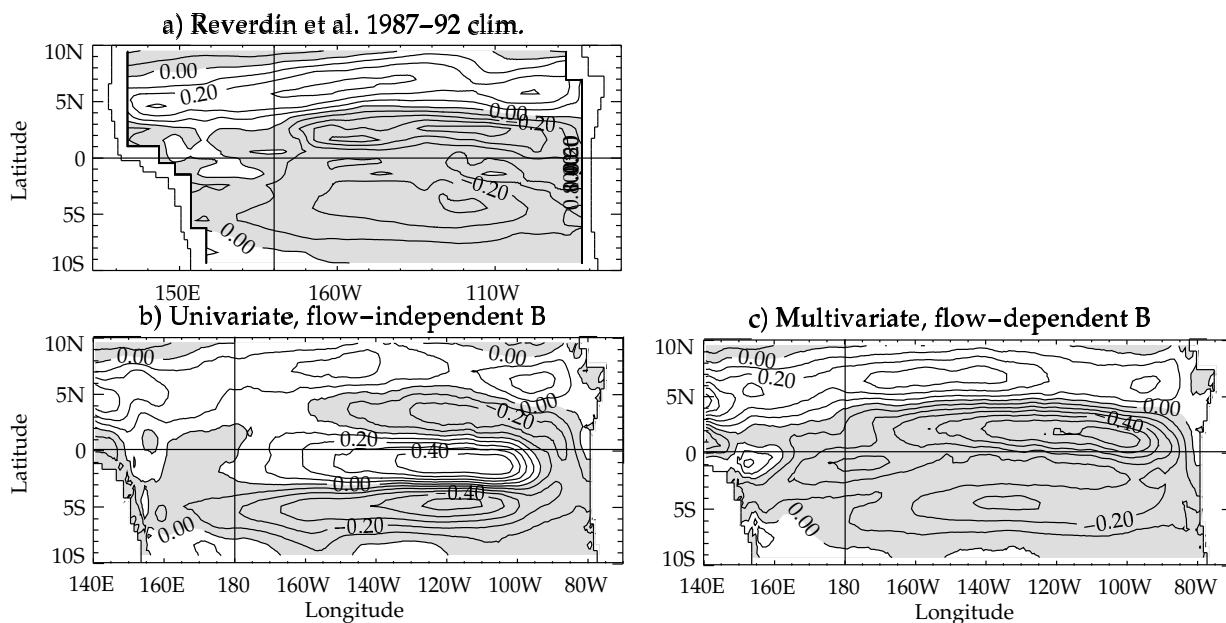
Acknowledgements

Figure 6: Surface zonal current climatologies. a) The Reverdin et al. (1994) climatology. Climatologies from 3D-Var using existing and improved formulations of **B***: a) univariate, flow-independent* **B***; and b) multivariate, flow-dependent* **B***. The contour interval is* $0.1ms^{-1}$*, and the shaded regions indicate westward currents.*

References

Balmaseda, M. A., 2003: Dealing with systematic error. *this issue*.

Bell, M. J., Forbes, R. M. and Hines, A., 2000: Assessment of the FOAM global data assimilation system for real-time operational ocean forecasting. *J. Mar. Syst.*, **24**, 249-275.

Bloom, S. C., Takacs, L. L., Da Silva, A. M. and Ledvina, D., 1996: Data assimilation using incremental analysis updates. *Mon. Wea. Rev.*, **124**, 1256–1271.

Burgers, G., Balmaseda, M. A., Vossepoel, F. C., van Oldenborgh, G. J. and van Leeuwen, P. J., 2002: Balanced ocean-data assimilation near the equator. *J. Phys. Oceanogr.*, **32**, 2509–2519.

Courtier, P., Thépaut, J.-N. and Hollingsworth, A., 1994: A strategy for operational implementation of 4D-Var, using an incremental approach. *Q. J. R. Meteorol. Soc.*, **120**, 1367–1388.

Courtier, P., Andersson, E., Heckley, W., Pailleux, J., Vasiljević, D, Hamrud, M., Hollingsworth, A., Rabier, F. and Fisher, M., 1998: The ECMWF implementation of three dimensional variational assimilation (3D-Var). Part I: Formulation. *Q. J. R. Meteorol. Soc.*, **124**, 1783–1808.

De Mey P. M. and Benkiran, M. 2001 : A multivariate reduced-order optimal interpolation method and its application to the Mediterranean basin-scale circulation. In *Ocean Forecasting: Conceptual basis and applications*, N. Pinardi, Ed., Springer-Verlag.

Fisher, M. and Andersson, E., 2001: Developments in 4D-Var and Kalman Filtering, ECMWF Tech. Memo. No. 347.

Gandin, L. S., 1965: *Objective analysis of meteorological fields*. Israeli Program for Scientific Translations, 242 pp.

Gauthier, P., Charette, C., Fillion, L., Koclas, P. and Laroche, S., 1999: Implementation of a 3D variational data assimilation system at the Canadian Meteorological Centre. Part 1: the global analysis. *Atmosphere-Ocean*, **37**, 103-156.

Hollingsworth, A. and Lönnberg, P., 1989: The verification of objective analyses: diagnostics of analysis system performance. *Meteorol. Atmos.*, **40**, 3–27.

Lorenc, A. C., 1981: A global three-dimensional multivariate statistical interpolation scheme. *Mon. Wea. Rev.*, **109**, 701–721.

Lorenc, A. C., Ballard, S. P., Bell, R. S., Ingleby, N. B., Andrews, P. L. F., Barker, D. M., Bray, J. R., Clayton, A. M., Dalby, T., Li, D., Payne, T. J. and Saunders, F. W., 2000: The Met. Office global three-dimensional variational data assimilation scheme. *Q. J. R. Meteorol. Soc.*, **126**, 2991–3012.

Madec, G., Delecluse, P., Imbard, M. and Levy, C., 1998: OPA 8.1 Ocean General Circulation Model Reference Manual. Technical note no. 11, LODYC/IPSL, Paris, France.

Nocedal, J. and Wright, S. J., 1999: *Numerical optimization.* Springer-Verlag. 636 pp.

Parrish, D. F. and J. C. Derber, 1992: The National Meteorological Center's spectral statistical interpolation analysis system. *Mon. Wea. Rev.*, **120**, 1747–1763.

Rabier, F., Järvinen, H., Klinker, E., Mahfouf, J.-F. and Simmons, A., 2000: The ECMWF operational implementation of four dimensional variational assimilation. Part I: Experimental results with simplified physics. *Q. J. R. Meteorol. Soc.*, **126**, 1143–1170.

Reverdin, G., Frankignoul, E., Kestenare, E. and McPhaden, M. J., 1994: Seasonal variability in the surface currents of the equatorial Pacific *J. Geophys. Res.*, **99**, 20323–20344.

Rutherford, I., 1972: Data assimilation by statistical interpolation of forecast error fields. *J. Atmos. Sci.*, **29**, 809–815.

Segschneider, J., Anderson, D. L. T., Vialard, J., Balmaseda, M. and Stockdale, T. N., 2002: Initialization of seasonal forecasts assimilating sea level and temperature observations. *J. Climate*, **14**, 4292–4307.

Smith, N. R., Blomley, J. E. and Meyers, G., 1991: A univariate statistical interpolation scheme for subsurface thermal analyses in the tropical oceans. *Prog. Oceanogr.*, **28**, 219–256.

Thépaut, J.-N., Courtier, P., Belaud, G. and LeMaître, G., 1996: Dynamical structure functions in a four-dimensional variational assimilation: a case study. *Q. J. R. Meteorol. Soc.*, **122**, 535–561.

Troccoli, A., Alonso Balmaseda, M., Segschneider, J., Vialard, J., Anderson, D. L. T., Stockdale, T., Haines, K. and Fox, A. D., 2002: Salinity adjustments in the presence of temperature data assimilation. *Mon. Wea. Rev.*, **130**, 89–102.

Vialard, J., Menkes, C., Boulanger, J.-P., Delecluse, P., Guilyardi, E., McPhaden, M. J. and Madec, G., 2001: A model study of oceanic mechanisms affecting equatorial Pacific sea surface temperature during the 1997-98 El Niño. *J. Phys. Oceanogr.*, **31**, 1649–1675.

Vialard, J., Weaver, A. T., Anderson, D. L. T. and Delecluse, P., 2003: Three- and four-dimensional variational assimilation with an ocean general circulation model of the tropical Pacific Ocean. Part 2: physical validation. *Mon. Wea. Rev.*, **131**, 1379–1395.

Weaver, A. T., Vialard, J. and Anderson, D. L. T., 2003: Three- and four-dimensional variational assimilation with an ocean general circulation model of the tropical Pacific Ocean. Part 1: formulation, internal diagnostics and consistency checks. *Mon. Wea. Rev.*, **131**, 1360–1378.